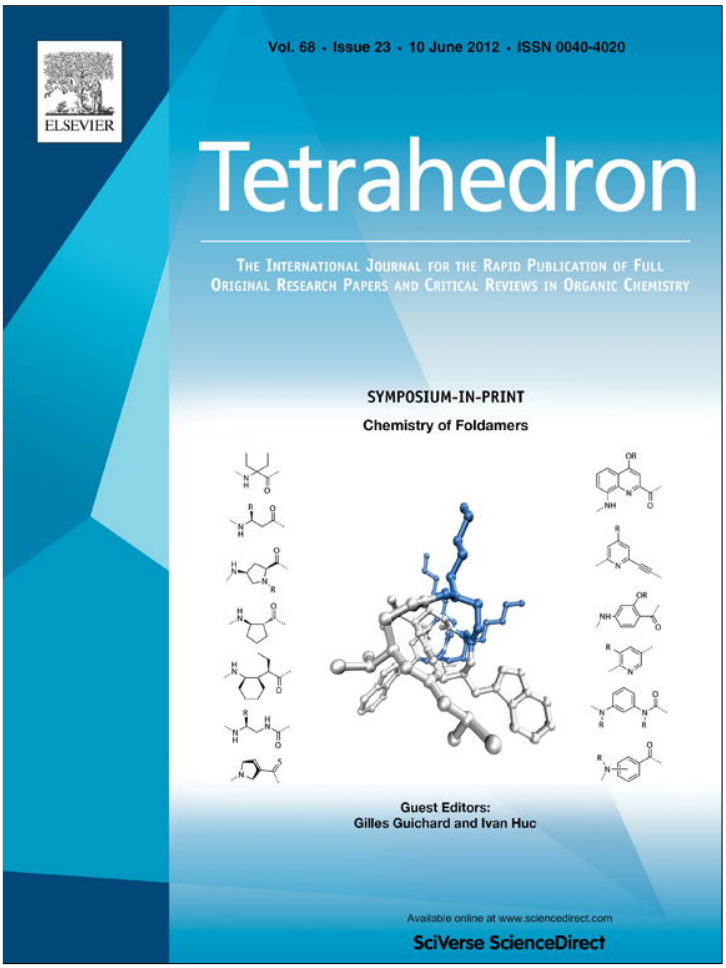

Tetrahedron 68 (2012) 4464–4469

Contents lists available at SciVerse ScienceDirect

Tetrahedron

journal homepage: www.elsevier.com/locate/tet

Assessing the folding propensity of aliphatic units within helical aromatic oligoamide foldamers

Nicolas Delsuc [a], Legiso Poniman [a], Jean-Michel Léger [b], Ivan Huc [a,*]

[a] Univ. Bordeaux—CNRS—IPB UMR5248, Institut Européen de Chimie et Biologie, 2 rue Robert Escarpit, 33607 Pessac, France
[b] Univ. Bordeaux—CNRS FRE 3396, 146 rue Léo Saignat, 33076 Bordeaux, France

ARTICLE INFO

Article history:
Received 2 November 2011
Received in revised form 25 November 2011
Accepted 30 November 2011
Available online 8 December 2011

Keywords:
Foldamers
Helical structures
Structure elucidation
Supramolecular chemistry
X-raydiffraction

ABSTRACT

Great attention is devoted to hybrid foldamers composed of more than one type of monomers. The folding of such hybrids requires units that may possess very different structures to be compatible. A method to assess this compatibility consists in studying the behavior of a monomer of one type within a sequence of another type of monomer. We have prepared and investigated the structure of flexible aliphatic monomers in the context of the rigid helices of quinoline-carboxamides. NMR and X-ray crystallography show that the rigid helical backbones may impart defined conformation into otherwise flexible units and that compatible folding modes exist between very different monomers.

1. Introduction

During the last decade, oligomeric strands able to adopt well defined folded conformations, i.e., foldamers, have been the object of increasing attention.[1] This interest stems from the long term hope that foldamers may mimic the functions of proteins or nucleic acids, which rest mostly on their ability to fold into defined structures, and also from the prospect that foldamers may give access to structures and functions beyond the reach of biopolymers. Thus, structurally diverse synthetic oligomers have been shown to adopt folded conformations, some of which having backbones and folding principles akin to those of biopolymers (biotic foldamers), others being more remote (abiotic foldamers). A majority of foldamer structures are secondary folded motifs, but artificial tertiary-like and quaternary structures have also began to appear.[2]

Like their natural counterparts, the first generations of foldamers generally consisted of a constant main chain repeat unit and variable side chains. The folded structures of these homologous oligomers were found to much resemble those of biopolymers (helices, linear strands and turns). However, during the last few years, a growing number of investigations focused on oligomers combining different monomers in the same sequence.[3] Hybrid oligomers composed of combinations of different aliphatic amino-acid units (e.g., α, β, and γ-amino-acids) have given rise to a variety of helical conformations that are similar to those of peptides but that differ in their side chains distribution.[4] This allows a fine-tuning of the functional groups arrangement at the helix surface depending on the synthetic amino-acid set chosen. Hybrids of aliphatic and aromatic units have also been explored.[5] Interestingly, the alternation of flexible aliphatic segments and more rigid aromatic units in these oligomers was sometimes found to produce unusual folding patterns such as knots,[6] 'tail biters',[7] pillars.[5a,8] For example, we have demonstrated that an alternated sequence of two δ-amino acids: 8-amino-2-quinolinecarboxylic acid (Q, aromatic) and 6-aminomethyl-2-pyridinecarboxylic acid (P, aliphatic) gave rise to a non-canonical helical conformation resembling a herringbone motif.[5b] Nevertheless, it was also shown that aromatic units may impose their folding behavior to multiple contiguous or non contiguous aliphatic units provided the former are in sufficient number.[5c] Upon adjusting the balance and sequence of aromatic and aliphatic residues, helices of identical length but with different stabilities were designed.

These recent developments suggest that hybrid sequences represent a rich and largely unexplored area. Innumerable combinations of monomers are accessible to synthesis. As a prime design element, the emergence of a defined folded motif in a hybrid sequence rests on the structural compatibility between at least two different units. For example, in the case of the P and Q units mentioned above, two distinct conformations of P were observed depending on the ratio between P and Q units. There is thus much

* Corresponding author. Fax: +33 540002215; e-mail address: i.huc@iecb.u-bordeaux.fr (I. Huc).

0040-4020/$ – see front matter © 2011 Elsevier Ltd. All rights reserved.
doi:10.1016/j.tet.2011.11.097

interest in exploring how several monomer types may combine their conformational preferences and give access to new folded structures. A method to explore the folding propensity of combinations of monomers consists in inserting one or a few monomers of one type into a well behaved sequence of another monomer type. The method also requires a reporter system of the eventual conformational changes that follow the introduction of the new monomers. Important progress along these lines have been proposed by Clayden and co-workers who developed an inducer/reporter system to investigate the perturbation of absolute helix handedness following the introduction of flexible units within an α-helix.[9] As another example, we have shown that the effect of inserting one new, e.g., aliphatic, unit between two well defined Q_n helical segments can be assessed by measuring the extent to which the handedness of the two helix segments communicate through the additional unit.[10] Depending on the conformation behavior of the additional unit, the handedness of one segment, e.g., *P* (right-handed), may be conveyed to the other segment, which would become *P* as well; it may be reverted at the other segment, which would then become *M* (left-handed);[11] or it may be interrupted, the other segment being indifferently *P* or *M*.

This strategy has been successfully applied to compound **4** (Fig. 1) and it was demonstrated by NMR and X-ray crystallography that a *meta m*-xylyl–diamine unit has no propensity to adopt the helical structure of Q_n oligomers in $CDCl_3$ but, on the contrary, that it folds well in toluene-d_8.[10] In the present manuscript, we have used the same methodology to investigate the folding propensity of other aliphatic units, which differ in nature, size, and flexibility: 1,2-ethylenediamine, 1,7-diaza-diethyleneglycol, and *p*-xylyl-diamine. The diamines were incorporated between two tetrameric segments Q_4, each undergoing a 1.5 helix turn with *M* or *P* handedness (Fig. 1). The proportions between the resulting racemate *PP*/*MM* on one hand and the degenerate *PM meso* species on the other hand are directly correlated to the helix propensity of the included aliphatic unit: a unit having a high helix propensity will transmit helix handedness from one helix segment to the other leading to the prevalence of the *PP*/*MM* species. Conversely, a unit having low helix propensity will result in a statistical mixture of *PP*/*MM* and *PM* species. Our results show that rather flexible units may exhibit high helix folding propensity once inserted in the context of Q_n oligomers. On the contrary, a semi-rigid unit may completely interrupt handedness communication when its structure is not compatible with the Q_n helices.

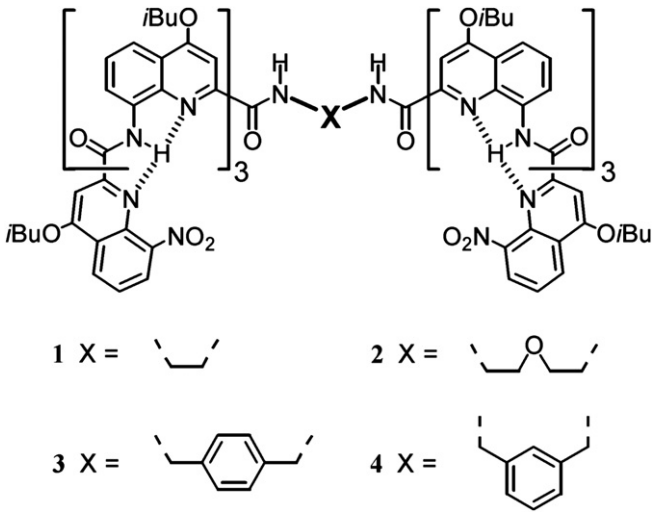

Fig. 1. Structures of oligomers **1**–**4**. Dashed lines represent intramolecular hydrogen bounds that participate to the helix stability.

2. Results and discussion

2.1. Synthesis

Oligomers **1**–**3** were synthesized in one step starting from a previously described tetrameric quinoline oligoamide with a free carboxylic acid C-terminus[12] and from commercially available diamines. The carboxylic acid was activated by a standard peptide coupling reagent (HBTU/HOBT) and coupling proceeded smoothly under basic conditions. After purification using silica-gel chromatography, the expected products were obtained in unoptimized yields ranging from 40 to 45%. Steric hindrance around the carboxylic acid function in the folded conformations may be responsible for these moderate yields.

2.2. Conformation of ethylenediamine bridged oligomer 1

The conformation of oligomer **1** was studied in solution by ^1H NMR in $CDCl_3$. At room temperature, the equilibrium between *PP*/*MM* and *PM* species is fast on the NMR time scale, leading to one set of signals (Fig. 2a). Three degenerate signals for aromatic amide protons are observed for the six protons of the full sequence. On average, the structure adopts a symmetry element, which reduces the multiplicity of NMR signals: a C_2 axis for *PP*/*MM* conformers or an inversion center for the *meso PM* species. Upon cooling to −30 °C, the equilibrium between the two species becomes slow on the NMR time scale and splitting into two sets of sharp signals with very distinct proportions was observed (Fig. 2c): 95% for the main species and 5% for the minor one. The amide resonances of the major species are shifted upfield from those of the minor species, indicating stronger ring current effects due to intramolecular aromatic stacking. X-ray crystallography (see below) and modeling studies suggest that extensive intramolecular aromatic stacking may occur only in the *PP*/*MM* conformer and thus that this species dominates in $CDCl_3$ solutions. In toluene-d_8 at −30 °C slow exchange is also reached as indicated by the diastereotopic pattern of the methylene protons of isobutoxy side chain, but only one set of signal is observed showing a strong preference for one conformer. NMR spectra measured in solvent mixtures show that the dominant species is the same (*PP*/*MM*) in $CDCl_3$ and toluene-d_8. Thus, the effect of intramolecular aromatic stacking to favor the *PP*/*MM* conformers is stronger in toluene than in $CDCl_3$, in agreement with results previously reported for compound **4**.[10]

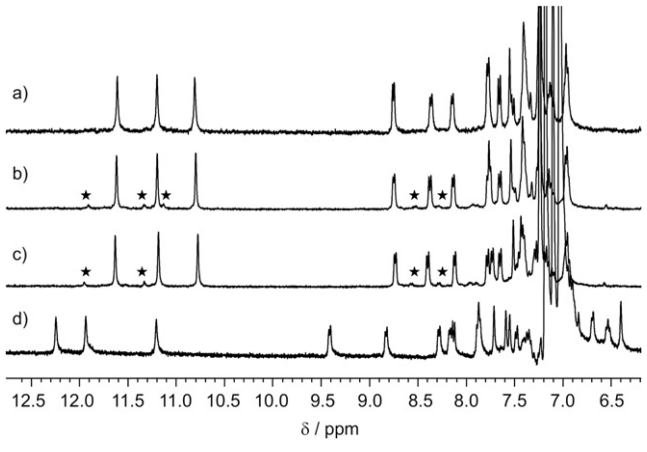

Fig. 2. Part of the 400 MHz ^1H NMR spectra of oligomer **1** showing amide and aromatic resonances in $CDCl_3$ at (a) 25 °C; (b) 0 °C; (c) −30 °C; and (d) in toluene-d_8 at −30 °C. Stars mark signals belonging to the PM species.

Single crystal X-ray crystallography allowed us to solve the structure of **1** in the solid state (Fig. 3). It corresponds to the PP/MM racemic species in which the ethylenediamine bridge adopts a *gauche* conformation. One might have expected that the large volume of the two helical segments carried by the ethylene bridge would disfavor a *gauche* conformation. Instead, this conformation permits extensive aromatic stacking to take place between the two helices and generates a compact object. Examination of molecular models suggests that no such stacking occurs in the trans conformation nor when the two helices have opposite handedness.

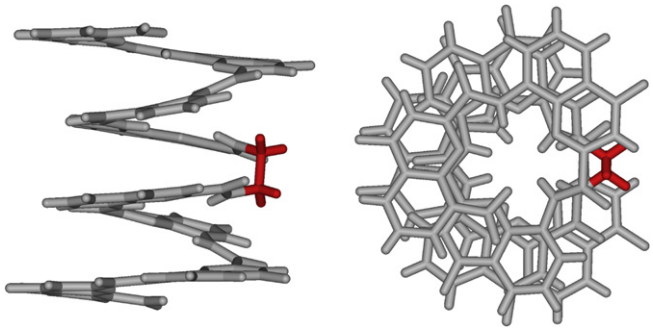

Fig. 3. Side view and top view of the crystal structure of oligomer **1** (*PP* conformer) showing the *gauche* conformation of the ethylene bridge. Isobutyl side chains and included solvent molecules have been omitted for clarity.

In order to bring unequivocal evidence that the solid state conformation is indeed the dominant species in solution, we attempted to measure the NMR spectrum of freshly dissolved crystals of **1**. However, equilibrium between the two species was reached during the course of the NMR spectrum's acquisition preventing an unambiguous assignment. Nevertheless, the results above all strongly suggest that the *PP*/*MM* helices dominate in solution and thus that the ethylenediamine unit has a high propensity to adopt a folded conformation compatible with quinolinecarboxamide helices.

2.3. Conformation of 1,7-diaza-diethyleneglycol bridged oligomer 2

Oligomer **2** was also studied by ^{1}H NMR. At room temperature in $CDCl_3$, its spectrum exhibits broad signals meaning that coalescence is reached (Fig. 4a). At −10 °C, the equilibrium between *PP*/*MM* and *PM* species is slow on the NMR time scale, and the signals split into two sets of sharp signals with different proportions (78/22). The species that predominates is again the one that possesses upfield-shifted signals, suggesting stronger ring current effects, i.e., more extensive π–π stacking. It was thus hypothesized again that this species corresponds to the fully folded PP/MM conformers. In toluene-d_8, **2** behaves similarly: broad signals are observed at 25 °C that sharpened upon cooling. However, the signals did not split into two sets of signals, revealing that only one conformation is present in solution. As for **1**, toluene-d_8 strongly favors one species, presumably the *PP*/*MM* conformers.

The solid state structure of **2** was obtained from crystals grown by slow diffusion of heptane in a dichloroethane solution. It shows the *PP*/*MM* conformers in which the diethyleneglycol bridge nicely aligns itself with the helix backbone (Fig. 5). This is allowed by a *gauche* conformation of both ethylene–glycol units. Intramolecular hydrogen-bonds between the central oxygen of the bridge and the two amide protons from the first quinoline unit at both sides presumably stabilize the structure. In consequence, the aliphatic unit is well inserted into the helical motif and transmits the helix handedness from one aromatic amide segment to the other. As for **1**, a *gauche* to trans conformational change may be

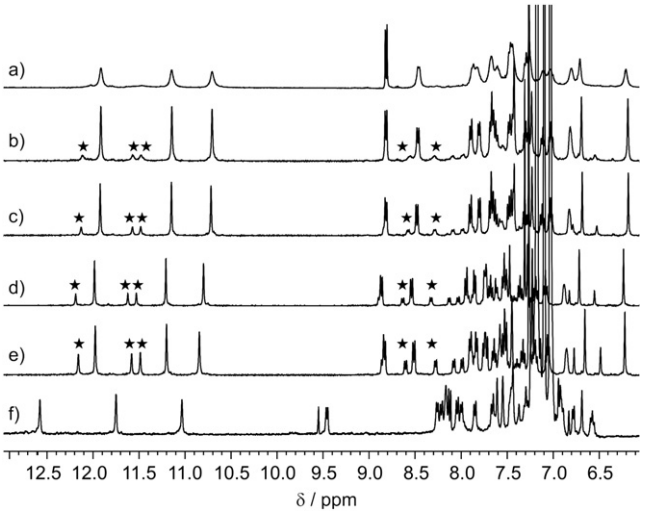

Fig. 4. Part of the 400 MHz ^{1}H NMR spectra of oligomer **2** showing amide and aromatic resonances in $CDCl_3$ at (a) 25 °C; (b) 0 °C; (c) −10 °C; (d) −20 °C; (e) −30 °C; and (f) in toluene-d_8 at −30 °C. Stars marks signals assigned to the minor species, which is presumably the PM species.

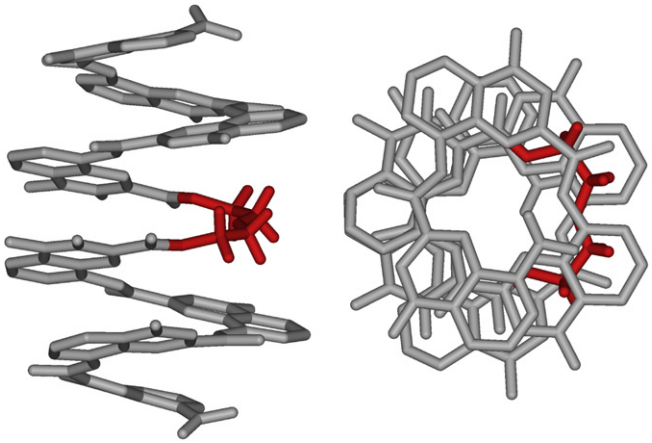

Fig. 5. Side view and top view of the crystal structure of oligomer **2** (*PP* conformer) showing the *gauche* conformation of the diethyleneglycol bridge. Isobutyl side chains and included solvent molecules have been omitted for clarity.

expected to occur in solution but it would result in the loss of intramolecular π–π stacking.

An interesting feature of oligomer **2** that was not observed with any other oligomer is that the proportions between the *PP*/*MM* and *PM* species are temperature dependant in $CDCl_3$: upon cooling from 0 °C to −30 °C, the proportions of the minor species increased from 19% to 32% (Fig. 4). It therefore appears that PP/MM is favored, but becomes less favored as temperature decreases. This effect is necessarily associated with the entropic component of the equilibrium, which could be calculated to be 43.5 J mol^{-1} from a Van't Hoff plot. It is nevertheless difficult to explain and may be associated with the solvation by water molecules of extended forms of the ethylene–glycol bridge in the PM conformer. Folding into the more compact PP/MM conformer would then cause the release of these molecules and be entropically favorable. No such effect was observed in toluene where only one species is detected.

2.4. Conformation of *p*-xylyl-diamine bridged oligomer 3

Whatever the solvent ($CDCl_3$ or toluene-d_8), the solution behavior of oligomer **3** was found to differ from those of **1** and **2**.

Below the coalescence temperature, the two sets of sharp signals corresponding to PP/MM and PM species of **3** are found in almost equal proportions (Fig. 6). This indicates that the free energy of helix reversal of a single segment is close to zero in this compound. In addition, the signals of the two species largely overlap, suggesting that the two helical segments on either side of the bridge are in similar environment regardless of their helix handedness. This would occur if the *p*-xylylene bridge interrupts helicity, preventing contacts between the two helical segments, which then behave independently. The conformation behavior of **3** may be compared to that of its *m*-xylylene isomer **4**, which we previously reported. In $CDCl_3$, **4** also shows equal proportions of the diastereomeric *PP*/*MM* and *PM* species but in toluene-d_8, the equilibrium was shifted to a ratio 9/1 in favor of the *PP*/*MM* conformers in which extensive intramolecular π–π stacking takes place.

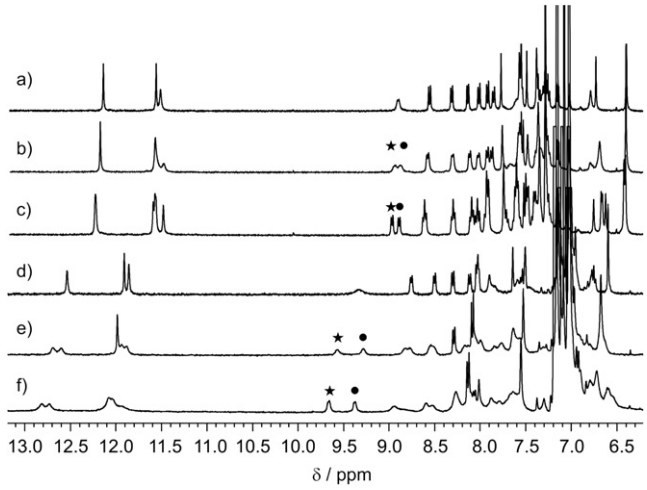

Fig. 6. Part of the 400 MHz ^{1}H NMR spectra of oligomer **3** showing amide and aromatic resonances in $CDCl_3$ at (a) 25 °C; (b) 0 °C; (c) −30 °C; and in toluene-d_8 at (d) 25 °C; (e) 0 °C; (f) −30 °C. Upon cooling in $CDCl_3$ or in toluene-d_8, signals split into two species marked with a circle or a star.

The structure of **3** was characterized in the solid state by X-ray diffraction analysis and it appeared that the crystals contained the *meso* species *PM* (Fig. 7). In this conformer, the phenyl ring of the bridge is almost perpendicular to the adjacent quinoline rings and is not involved in face-to-face aromatic stacking. This is in contrast with the structure of **4**, for which the *PP*/*MM* species crystallized, and in which the m-xylylene bridge lies flat between two quinoline rings (Fig. 7). The solid state conformation of **3** is thus less compact than that of **4**. The *para* substitution of the bridge imposes some distance between the helical segments, which prevents interactions between them in contrast to what occurs with the *meta* isomer. Therefore, the *p*-xylyl–diamine unit has no helix propensity in the context of quinolinecarboxamide oligomers.

3. Conclusion

The results reported above show that relatively simple and apparently flexible aliphatic units, e.g., ethylene or diethyleneglycol, having no apparent reason to adopt folded conformations eventually fold once incorporated in the context of a rigid helically folded aromatic oligoamide. Solid state structures show that *gauche* conformations are imposed within these aliphatic units upon folding. Folding of the aliphatic units appears to be driven by intramolecular stacking between aromatic units. Thus, despite large structural differences, aliphatic and aromatic units may display surprising compatible behaviors with respect to folding. In contrast, due to its higher rigidity a *p*-xylyl unit may result in a local disruption of folding introducing two helical aromatic oligoamide segments, which behave independently. Overall, it appears that a great variety of different units may be combined at will within a foldamer sequence and that the chemical space of folded structures is far greater than suggested by the observation of the biopolymers backbones, which consist of a constant main chain repeat.

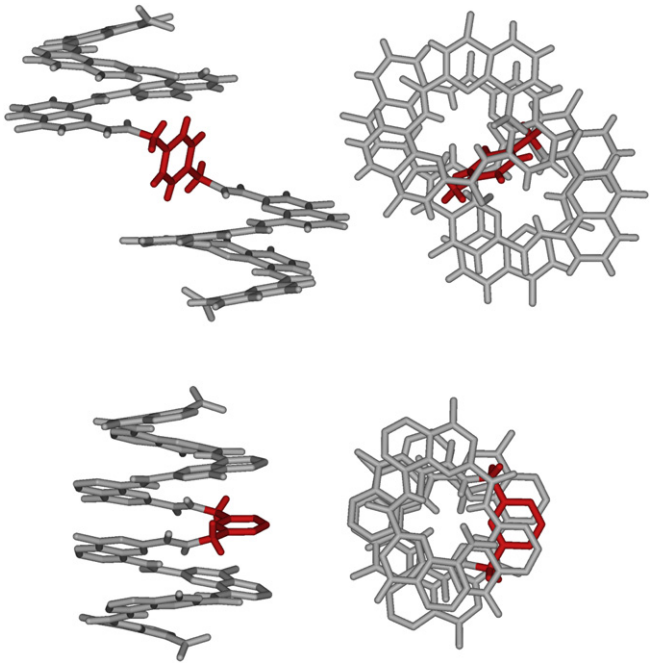

Fig. 7. Side view and top view of the crystal structures of oligomer **3** (top, *MP* conformer) and of oligomer **4** (bottom, *PP* conformer), at the same scale. Isobutyl side chains and included solvent molecules have been omitted for clarity.

4. Experimental section

4.1. Materials

Unless otherwise noted, materials were obtained from commercial suppliers and used without further purification. Diisopropylethylamine (DIPEA) and DMF were distilled from CaH_2 prior to use. Chemical shifts are reported in parts per milliom and are calibrated against residual solvent signals of $CDCl_3$ (δ 7.26, 77.0) or toluene-d_8 (δ 2.08, 20.4). All coupling constants are reported in hertz. Silica-gel chromatography was performed using Merck Kieselgel Si 60. NMR Spectra were recorded with a Bruker Avance 400 NB US NMR spectrometer by means of a 5 mm direct QNP 1H/X probe with gradient capabilities or on a Bruker 300 Avance. Matrix assisted laser desorption ionization time of flight (MALDI-TOF) mass spectra were obtained in positive ion mode using α-cyano-hydroxycinnamic acid as a matrix.

4.2. General procedure

The precursor quinoline tetramer acid (100 mg, 0.1 mmol, 2.05 equiv), HBTU (114 mg, 0.3 mmol, 3 equiv), and HOBt (27 mg, 0.2 mmol, 2 equiv) were dissolved in anhydrous DMF under nitrogen. DIEA (173 μL, 1 mmol, 10 equiv) was added and the reaction mixture was stirred at room temperature for 30 min. The diamine (1 equiv) was added and the reaction mixture was stirred at room temperature for 12 h. The reaction mixture was poured into water, extracted three times with toluene, dried over Na_2SO_4, filtered, and concentrated. The crude was purified by silica-gel chromatography

eluting with toluene/ethyl acetate 90/10 v/v, yielding the expected compound as a yellow solid.

4.2.1. Oligomer ***1***. Yield: 65%, yellow solid; δ_H (400 MHz $CDCl_3$ 25 °C) 11.56 (1H, s), 11.15 (1H, s), 10.77 (1H, s), 8.75 (1H, d, *J*=7.3 Hz), 8.73 (1H, s), 8.37 (1H, s), 8.16 (1H, s), 8.14 (1H, s), 7.79 (1H, s), 7.77 (1H, d, *J*=4.6 Hz), 7.68 (1H, d, *J*=4.6 Hz), 7.66 (4H, m), 7.09 (1H, s), 7.07 (1H, s), 7.06 (1H, s), 6.97 (1H, t, *J*=8.2 Hz), 6.92 (1H, t, *J*=8.2 Hz), 6.56 (1H, s), 6.53 (1H, s), 6.52 (2H, m), 6.50 (1H, s), 6.45 (1H, s), 6.35 (2H, m), 6.31 (1H, s), 6.26 (1H, s), 6.15 (1H, s), 6.12 (1H, s), 5.93 (1H, d, *J*=7.2 Hz), 5.92 (1H, s), 5.88 (1H, s), 5.87 (1H, d, *J*=7.2 Hz), 5.74 (2H, t, *J*=7.5 Hz), 4.25–3.45 (32H, m), 2.71 (2H, t, *J*=13.2 Hz), 2.57–2.13 (16H, m), 1.45–0.82 (96H, m); ν_{max} (liquid film) 3318, 2959, 2918, 2873, 2849, 1686, 1592, 1571, 1560, 1540, 1535, 1508, 1502, 1492, 1484, 1467, 1460, 1453, 1419, 1383, 1357, 1330, 1262, 1211, 1115, 1054 cm^{-1}; HRMS (ESI): MH^+, found 2057.8685. $C_{114}H_{117}N_{18}O_{20}$ requires 2057.8691.

4.2.2. Oligomer ***2***. Yield :42%, yellow solid; δ_H (400 MHz $CDCl_3$ 25 °C) 11.34 (1H, s), 11.20 (1H, s), 11.12 (1H,s), 8.32 (1H, d, *J*=8.0 Hz), 8.19 (1H, d, *J*=7.5 Hz), 7.80 (2H, m), 7.54 (1H, s), 7.47 (1H, d, *J*=7.4 Hz), 7.40 (1H, d, *J*=8.3 Hz), 7.30 (1H, d, *J*=8.3 Hz), 7.21 (1H, d, *J*=7.4 Hz), 7.17–7.08 (4H, m), 7.09 (1H, t, *J*=8.0 Hz), 7.04 (1H, t, *J*=8.0 Hz), 6.51 (1H, s), 6.35 (1H, s), 4.28 (1H, t, *J*=7.4 Hz), 4.15 (1H, t, *J*=6.9 Hz), 4.11 (1H, t, *J*=6.9 Hz), 4.05 (1H, t, *J*=8.0 Hz), 4.03 (1H, t, *J*=8.3 Hz), 3.88 (1H, t, *J*=7.4 Hz), 3.84 (1H, t, *J*=7.4 Hz), 3.74 (1H, t, *J*=7.4 Hz), 2.50–2.25 (4H, m), 1.41–1.14 (24H, m); δ_C (100 MHz $CDCl_3$ 25 °C) 158.3, 158.0, 157.9, 157.6, 156.7, 156.0, 153.2, 151.2, 149.0, 146.3, 144.4, 140.2, 139.8, 139.3, 133.5, 133.4, 133.3, 129.1, 129.0, 128.3, 122.0, 121.4, 121.8, 119.3, 117.6, 116.3, 116.0, 112.8, 112.1, 112.0, 111.8, 111.8, 96.4, 95.9, 95.8, 93.3, 71.3, 71.1, 70.7, 24.2, 24.1, 24.0, 15.5, 15.4, 15.3, 15.2; ν_{max} (liquid film) 2961, 2931, 2874, 1792, 1682, 1642, 1625, 1591, 1570, 1540, 1535, 1508, 1469, 1420, 1399, 1384, 1356, 1343, 1331, 1264, 1215, 1163, 1117, 1077, 1062, 1050, 1040 cm^{-1}; HRMS (ESI): MH^+, found 2101.8947. $C_{116}H_{121}N_{18}O_{21}$ requires 2101.8953.

4.2.3. Oligomer ***3***. Yield: 45% yellow solid; δ_H (400 MHz $CDCl_3$ 25 °C) 11.95 (1H, broad), 11.43 (1H, s), 11.35 (1H, broad), 8.73 (1H, broad), 8.43 (1H, d, *J*=8.0 Hz), 8.15 (1H, broad), 8.02 (1H, d, *J*=7.4 Hz), 7.88 (1H, d, *J*=8.2 Hz), 7.80 (1H, d, *J*=7.8 Hz), 7.76 (1H, d, *J*=8.2 Hz), 7.62 (1H, large), 7.52 (1H, t, *J*=8.1 Hz), 7.44 (1H, t, *J*=7.8 Hz), 7.36 (1H, s), 7.31 (1H, large), 7.25 (1H, t, *J*=7.9 Hz), 7.17 (1H, d, *J*=7.3 Hz), 7.15 (1H, t, *J*=7.8 Hz), 6.68 (1H, s), 6.62 (1H, s), 6.43 (1H, large), 6.26 (1H, large), 5.94 (1H, t, *J*=7.6 Hz), 4.35–3.63 (8H, m), 2.45–2.07 (4H, m), 1.25–0.93 (24H, m). δ_C (100 MHz $CDCl_3$ 25 °C) 159.8, 158.8, 158.7, 158.4, 158.3, 157.9, 157.1, 156.3, 149.4, 146.7, 144.8, 144.3, 141.1, 134.8, 134.7, 134.0, 133.9, 133.1, 130.4, 129.3, 128.9, 123.6, 123.4, 122.3, 122.0, 121.4, 119.9, 119.6, 118.1, 117.7, 117.5, 113.8, 112.8, 112.7, 112.4, 112.2, 111.6, 96.1, 94.5, 94.3, 93.6, 71.5, 71.2, 70.9, 70.8, 24.0, 23.9, 15.1, 15.0; ν_{max} (liquid film) 2961, 2931, 2874, 1685, 1648, 1637, 1618, 1591, 1570, 1540, 1535, 1507, 1469, 1420, 1398, 1384, 1358, 1330, 1301, 1263, 1213, 1163, 1116, 1051 cm^{-1}; HRMS (ESI): MH^+, found 2133.9014. $C_{120}H_{121}N_{18}O_{20}$ requires 2133.9004.

4.3. X-ray crystallography

Single crystals of **1**–**3** were mounted on a Rigaku R-Axis Rapid diffractometer equipped with an MM07 microfocus rotating anode generator (monochromatized Cu κα radiation, 1.54178 Å). The data collection, unit cell refinement, and data reduction were performed by using the CrystalClear® software package. The position of non-H atoms were determined by the program SHELXD and refined with SHELXH. The position of the H atoms were deduced from coordinates of the non-H atoms and confirmed by Fourrier synthesis. H atoms were included for structure factor calculations but not refined. Crystallographic parameter are reported in Table 1.

Table 1
Crystallographic data for **1**–**3**

	1	**2**	**3**
Solvent–precipitant	Dimethylsulfoxide–methanol	Dichloroethane–heptane	Benzene–heptane
Formula (asymmetric unit)	$(C_{57}H_{58}N_9O_{10})$ (H_2O) $(CH_4O)_{1.25}$ $(C_2H_6OS)_{0.75}$	$(C_{118}H_{119}N_{17}O_{22})$	$C_{120}H_{120}N_{18}O_{20}(H_2O)$ $(C_6H_6)_2$
Aspect	Yellow prism	Yellow prism	Yellow prism
Cryst syst.	Monoclinic	Monoclinic	Triclinic
Space group	*C*2/*c*	*C*2/*c*	*P*−1
Z	8	8	2
Unit cell param.			
a (Å)	32.1171(17)	32.7650(10)	15.5977(2)
b (Å)	21.4790(10)	24.3810(10)	16.1710(4)
c (Å)	20.6782(10)	33.0880(10)	25.5202(5)
α (°)	90	90	85.663(4)
β (°)	124.445(3)	120.746(3)	74.101(3)
Γ (°)	90	90	82.640(3)
Temp (K)	213(2)	173(2)	213(2)
Volume ($Å^3$)	11,763.7(10)	22,716.9(13)	6134.2(2)
Fw ($g\ mol^{-1}$)	1144.84	2162.75	2308.57
ρ ($g\ cm^{-3}$)	1.293	1.265	1.250
Radiation	Cu Kα	Cu Kα	Cu Kα
λ (Å)	1.54178	1.54178	1.54178
θ measured	6.55–72.24	6.51–72.32	6.42–72.12
Refl. measured	81,422	151,689	70,107
Refl. Unique	10,898	21,411	21,490
GOF	1.091	1.039	1.069
R_1 ($I>2\sigma(I)$)	0.0785	0.1224	0.2532
wR_2 (all data)	0.2407	0.4033	0.7127
CCDC#	851346	851347	851348

Acknowledgements

This work was supported by the French Ministry of Research (Predoctoral fellowship to N.D.) and by the Asian Bank of Development (Predoctoral fellowship to L.P.). We thank Dr. Brice Kauffmann for assistance with X-ray data collection.

Supplementary data

Supplementary data related to this article can be found online at doi:10.1016/j.tet.2011.11.097.

References and notes

1. (a) *Foldamers: Structure, Properties and Applications*; Hecht, S., Huc, I., Eds.; Wiley-VCH: Weinheim, 2007; (b) Guichard, G.; Huc, I. *Chem. Commun.* **2011**, 5933.
2. (a) Delsuc, N.; Léger, J.-M.; Massip, S.; Huc, I. *Angew. Chem., Int. Ed.* **2007**, *46*, 214; (b) Delsuc, N.; Massip, S.; Léger, J.-M.; Kauffmann, B.; Huc, I. *J. Am. Chem. Soc.* **2011**, *133*, 3165; (c) Horne, W. S.; Price, J. L.; Keck, J. L.; Gellman, S. H. *J. Am. Chem. Soc.* **2007**, *129*, 4178; (d) Daniels, D. S.; Petersson, E. J.; Qiu, J. X.; Schepartz, A. *J. Am. Chem. Soc.* **2007**, *129*, 1532.
3. Roy, A.; Prabhakaran, P.; Kumar Baruah, P.; Sanjayan, G. *J. Chem. Commun.* **2011**, *47*, 11593.
4. (a) Horne, W. S.; Gellman, S. H. *Acc. Chem. Res.* **2008**, *41*, 1399; (b) Vasudev, P. G.; Chatterjee, S.; Shamala, N.; Balaram, P. *Chem. Rev.* **2011**, *111*, 657; (c) Sharma, G. V.; Reddy, K. R.; Krishna, P. R.; Sankar, A. R.; Narsimulu, K.; Kumar, S. K.; Jayaprakash, P.; Jagannadh, B.; Kunwar, A. C. *J. Am. Chem. Soc.* **2003**, *125*, 13670; (d) Mándity, I. M.; Wéber, E.; Martinek, T. A.; Olajos, G.; Tóth, G. K.; Vass, E.; Fülöp, F. *Angew. Chem., Int. Ed.* **2009**, *48*, 2171; (e) Hetényi, A.; Tóth, G. K.; Somlai, C.; Vass, E.; Martinek, T. A.; Fülöp, F. *Chem.—Eur. J.* **2009**, *15*, 10736; (f) Claudon, P.; Violette, A.; Lamour, K.; Decossas, M.; Fournel, S.; Heurtault, B.; Godet, J.; Mély, Y.; Jamart-Grégoire, B.; Averlant-Petit, M.-C.; Briand, J.-P.; Duportail, G.; Monteil, H.; Guichard, G. *Angew. Chem., Int. Ed.* **2010**, *49*, 333.
5. (a) Lokey, R. S.; Iverson, B. L. *Nature* **1995**, *375*, 303; (b) Delsuc, N.; Godde, F.; Kauffmann, B.; Léger, J.-M.; Huc, I. *J. Am. Chem. Soc.* **2007**, *129*, 11348; (c) Sànchez-García, D.; Kauffmann, B.; Kawanami, T.; Ihara, H.; Takafuji, M.; Delville, M.-H.; Huc, I. *J. Am. Chem. Soc.* **2009**, *131*, 8642; (d) Prabhakaran, P.; Kale, S. S.; Puranik, V. G.; Rajamohanan, P. R.; Chetina, O.; Howard, J. A.; Hofmann, H. J.; Sanjayan, G. J. *J. Am. Chem. Soc.* **2008**, *130*, 17743.
6. (a) Brüggemann, J.; Bitter, S.; Müller, S.; Müller, W. M.; Müller, U.; Maier, N. M.; Lindner, W.; Vögtle, F. *Angew. Chem., Int. Ed.* **2006**, *46*, 254; (b) Feigel, M.; Ladberg, R.; Engels, S.; Herbst-Hirmer, R.; Fröhlich, R. *Angew. Chem., Int. Ed.* **2006**, *45*, 5698; (c) Boehmer, A.; Brüggemann, J.; Kaufmann, A.; Yoneva, A.; Müller, S.; Müller, W. M.; Müller, U.; Vergeer, F. W.; Chi, L.; De Cola, L.; Fuchs, H.; Chen, X.; Kubota, T.; Okamoto, Y.; Vögtle, F. *Eur. J. Org. Chem.* **2007**, *1*, 45.
7. Hunter, C. A.; Spitaleri, A.; Tomas, S. *Chem. Commun.* **2005**, 3691.
8. (a) Gabriel, G. J.; Sorey, S.; Iverson, B. L. *J. Am. Chem. Soc.* **2005**, *127*, 2637; (b) Ghosh, S.; Ramakrishnan, S. *Angew. Chem., Int. Ed.* **2004**, *43*, 3264; (c) Zhang, W.; Horoszewski, D.; Decatur, J.; Nuckolls, C. *J. Am. Chem. Soc.* **2003**, *125*, 4870; (d) Gabriel, G. J.; Iverson, B. L. *J. Am. Chem. Soc.* **2002**, *124*, 15174.
9. Clayden, J.; Castellanos, A.; Solà, J.; Morris, G. A. *Angew. Chem., Int. Ed.* **2009**, *48*, 5962.
10. Dolain, C.; Léger, J.-M.; Delsuc, N.; Gornitzka, H.; Huc, I. *Proc. Natl. Acad. Sci. U.S. A.* **2005**, *102*, 16146.
11. Maurizot, V.; Dolain, C.; Leydet, Y.; Léger, J.-M.; Guionneau, P.; Huc, I. *J. Am. Chem. Soc.* **2004**, *126*, 10049.
12. Jiang, H.; Léger, J.-M.; Huc, I. *J. Am. Chem. Soc.* **2003**, *125*, 3448.